ACS OMEGA

Article

Cite This: ACS Omega 2019, 4, 6979−6993

http://pubs.acs.org/journal/acsodf

A Study of the Effect of Kosmotropic and Chaotropic Ions on the Release Characteristics of Lignin Microcapsules under Stimuli-Responsive Conditions

Luc Zongo,[†] Heiko Lange,[†] and Claudia Crestini*[,‡]

[†]Department of Chemical Sciences and Technologies, University of Rome 'Tor Vergata', Via della Ricerca Scientifica 1, 00133 Rome, Italy

[‡]Department of Molecular Sciences and Nanosystems, University of Venice Ca' Foscari, Via Torino 155, 30170 Mestre, Venice, Italy

ABSTRACT: Stimuli-responsive behavior of lignin microcapsules (LMCs) has been investigated along with the detailed characterization of their stability profiles. The disassembly of LMCs was found to be salt species-dependent, indicating the specific relevance of inherent kosmotropic and chaotropic characteristics. For the first time, a connection between the Hofmeister series and the stability profile of lignin microscale materials is established. LMCs showed excellent stability in water and under high temperature and pressure (autoclaving conditions). Active release is efficiently triggered by pH changes and balancing chaotropic and kosmotropic effects via salinity tuning.

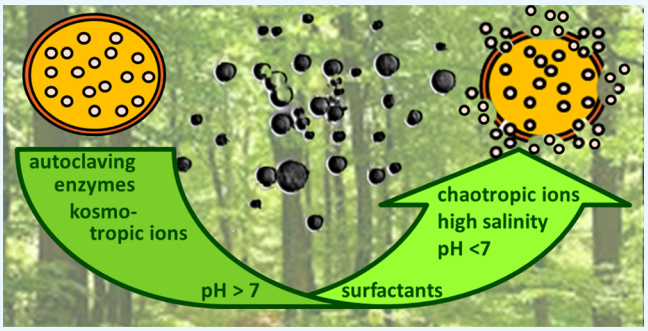

INTRODUCTION

The microencapsulation technique, a concept introduced by Chang in the 1960s,[1] can be defined as the process by which one compound is coated with another compound.[2,3] The coated component, or components in the case of mixtures of substances, can be an active agent, such as pesticides, poorly soluble drugs, flavors, or food additives.[4−7]

Nowadays, the microencapsulation process is of significant interest in academic and industrial research.[6−14] Relevant investigations in microencapsulation have been performed in the context of pharmaceutical and biomedical applications, such as drug delivery, cell implantation, and gene therapy, as well as applications in biotechnology such as fermentation and large-scale cell culture involving a variety of materials and preparation technologies.[12,15]

The intended purpose of the microencapsulation is the relevant criterion underlying the selection of the shell component.[3,6] The suitable shell component must be chemically compatible with the core material, to provide the desired coating properties, such as strength, flexibility, permeability, optical properties, and stability.[3] In this respect, lignins represent an interesting option.

Almost one third of lignocellulosic biomass comprises polyphenolic oligomers and polymers, which are for the most part lignins.[16−19] Lignins are naturally synthesized in vascular plants by the polymerization of phenylpropane units; the resulting polymers are structurally complex polyphenols. An even larger variety and diversity is caused by the fact that different wood species, in combination with variable extraction processes, result in different structural characteristics of available lignin species[20−23] (Figure 1). The valorization of lignin waste streams from pulp and paper and modern biorefinery processes is a crucial step for the development of a circular sustainable economy.

Lignosulfonates (LSs) are produced when biomass is pulped with a metal sulfite and sulfur dioxide under acidic conditions. The resulting LS fraction contains two types of ionizing groups: sulfonates ($pK_a \leq 2$) and phenolic hydroxyl groups ($pK_a \sim 10$). The physicochemical properties of LSs are affected by the metal cation of the sulfite salt used during the pulping process,[24] that is, Na(I) or Ca(II).

LSs are eco-friendly materials with a safety threshold of 10 kg/m^2, which is very much above the 1 kg/m^2 required for stabilization and the 0.3 kg/m^2 used for dust control; and residuals are resistant to decay.[25] LSs possess a very low toxicity toward plants[26] and aquatic animals.[27] Additionally, they are free of dioxins and other organics at hazardous levels, and their toxic trace minerals are below the Extraction Procedure Toxicity threshold according to United States Environmental Protection Agency.[25,28] The usefulness of commercial lignosulfonate products comes from their dispersing, binding, complexing, and emulsifying properties.[29] The additive calcium lignosulfonate as described in the Food Chemicals Codex[30] has been used for a number of years in the food industry,[26] serving, for example, as an emulsifier in animal feed, as a raw material in the production of vanillin, and as a boiler water additive.[29]

Received: December 14, 2018
Accepted: March 1, 2019
Published: April 18, 2019

DOI: 10.1021/acsomega.8b03510
ACS Omega 2019, 4, 6979−6993

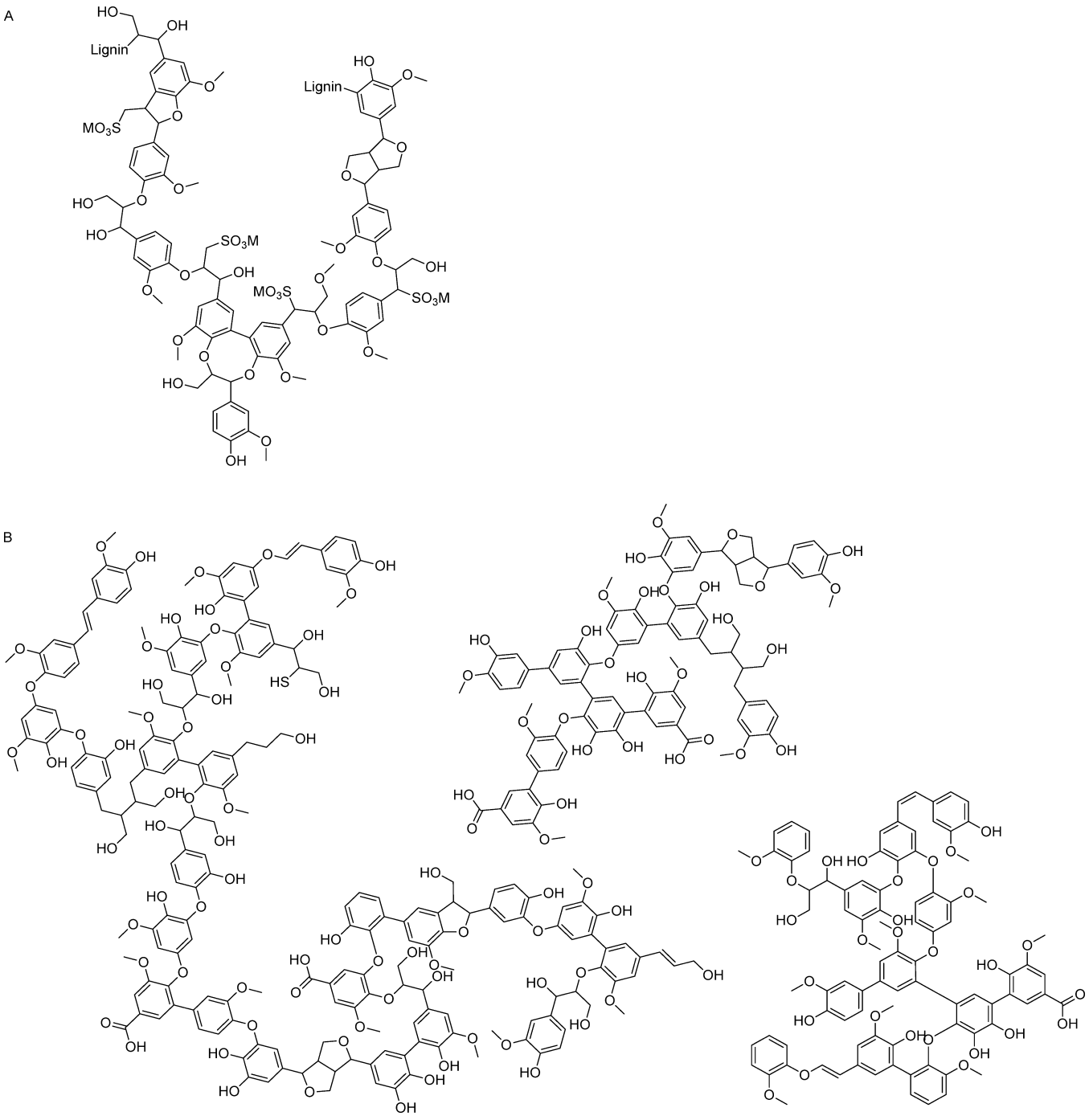

Figure 1. Structural examples for (A) softwood lignosulfonate[21] and (B) softwood kraft lignin.[31]

Other types of isolated lignins such as softwood kraft lignin (SKL) are also commercially available. SKL, in particular, is cost-effective as well as available in industrial quantities[22] and displays numerous beneficial properties as an LS.[10,16,31,32] Figure 1 shows exemplary structural representations of these two lignins. Depending on the targeted field of use, SKL might represent a valid alternative for the use of LSs.

Several studies demonstrated that lignins have useful rheological and viscoelastic properties to develop a structural material,[16,24,33] meaningful film forming ability,[31,33,34] and compatibility with a wide range of solvents.[23,24,34] Lignins are multifunctional biopolymers that carry many aliphatic hydroxyl and phenolic groups. Technical lignins additionally present sulfonate groups (SLS) or increased phenolic group contents and concomitant reduced contents of aliphatic chains (SKL). The abundance of different functional groups allows in principle for a broad range of chemical transformations[16,23,24,35] that can serve both to control reactivity in industrial applications[10,16,31,32,36] and modify physicochemical parameters such as surface adhesion properties or thermal stabilities. The presence of the aromatic functionality naturally provides stability, good mechanical properties, and amphiphilic characteristics. Lignins offer, in addition to the aforementioned properties, other significant features such as aggregation properties,[10,32,36] high biocompatibility, and ability to absorb UV light.[37] The intrinsic electronic stacking and complexing

DOI: 10.1021/acsomega.8b03510
ACS Omega 2019, 4, 6979−6993

Table 1. Assessment of SKL-MC and SLS-MC Stability after 180 Days

		mean Ø (μm)		PDI		number of LMCs (10^{12} LMCs/mL)		stability index	
entry	age of LMCs (days)	SLS	SKL	SLS	SKL	SLS	SKL	SLS	SKL
1	1	1.26	1.55	0.3	0.5	6.57	7.24	1.00	1.00
2	180	1.36	1.50	0.4	0.5	6.44	7.17	0.98	0.99

properties, as well as the possibilities for hydrophobic interactions, make lignins ideal matrixes for microencapsulation.[14,38] Interactions among lignin oligomers were shown to be fundamental for the generation of robust microcapsules via the sonochemical method.[10,14]

To be qualified for their potential applications, lignin microcapsules (LMCs) have to possess some particular characteristics, including a suitable stability and release profile at a specific site of interest or upon a specific type of chemical or physical trigger.

The present work was designed to achieve both, the development of a novel type of stimuli-responsive lignosulfonate (LS) microcapsules and a detailed mapping of their stability under various conditions in comparison to kraft lignin (KL) microcapsules. These two selected technical lignins, that is, a softwood-based lignosulfonate (SLS) and a softwood-based kraft lignin (SKL), were chosen on the basis of their significant difference in amphiphilic character and water solubility.

A Machiavellian assessment of the stability of microcapsules is necessary in case one is really interested in developing such structures for real-life applications with very different boundary conditions and pre-set parameters. Once formed and characterized, the study of stimuli-triggered LMC disassembly was thus realized using selected physical and chemical conditions, screening effects of time, temperature, pressure, pH, salinity, osmotic stress, physiologically important molecules, surfactant and solvents. Our study aimed at delineating interconnected effects, trying to determine which parameter, in case there are multiple effects present, is the determining one, such as to eventually get hints of how to alter basic LMCs to render them more suitable in specific settings. To guarantee overall comparability of the results, stability studies were performed in a very strictly standardized fashion: LMCs were evaluated by default after being subjected to test conditions for 24 or 48 h. The scope of this study was not to evaluate the kinetics of a potential capsule degeneration but, as a first step in LMC stability evaluation, to get a more universal idea of how LMCs are affected by specific physicochemical conditions. This study wants to lay the groundwork for eventual kinetic investigations under specific conditions pre-set by targeted applications.

RESULTS AND DISCUSSION

Conceptual Approach to Microcapsule Generation. When approaching the design of microcapsules, one has to take into consideration key issues such as biocompatibility, stability, tendency to aggregate − that is, stacking and complexing of the matrix − and amphiphilicity. In this study, the objective was the generation of biocompatible microcapsules. The choice of lignin as a possible matrix was due to its significant antioxidant activity. Such an intrinsic lignin property shows promising potential in protecting a sensitive loaded active ingredient from oxidative stress and degradation. To obtain robust lignin microcapsules, two lignins with different amphiphilicities, water solubilities, and pH-related behaviors were selected: SLS, which is rich in sulfonate and phenolic groups, and SKL, which is rich in phenolic groups. According to a previously reported procedure, the lignins were dissolved in water and, an oil-in-water emulsion was generated and subjected to ultrasonication. In brief, LMCs have been generated on a 1 mL scale from a 10:1 mixture of aqueous SKL solution (0.5% w/v) and olive oil treated by ultrasonication at 40 W (10% amplitude) for 40 s. The statistical quantitative analysis, using a combination of microscopy and ImageJ-based analysis, suggested a perfect stability over time in a neutral pH and salt-free aqueous environment, that is distilled water.[10]

For generating higher quantities of capsules as needed in this study, this procedure has been revisited and optimized by systematically varying the values of pH, lignin concentration, water/oil phases ratio, ultrasonication power, and time. As a result, a 1:1 mixture of an aqueous SKL solution (0.5% w/v) at pH ∼12 and the oily phase, firstly magnetically stirred for 5 min and subsequently treated by ultrasonication at 160 W (40% amplitude) for 10 min, was found to be the most efficient setup for the generation of lignin microcapsules. This approach results in a 5-fold increase of volume of isolated and "concentrated", that is, densely packed SKL microcapsules. Most noteworthy is that using these further optimized conditions, it was also possible for the first time to process and isolate microcapsules from SLS upon ultrasonication starting from oil-in-water emulsions.

Assessment of Robustness of LMCs: Time-Dependent Stability. Freshly made and 6 month-old SLS-MCs and SKL-MCs generated using the optimized setup display statistical quantitative characteristics that are de facto identical in the range of the average error determined for the chosen statistical quantitative analysis, as reported in Table 1. Consequently, the stability index, best defined as the ratio between the number of LMCs at day 1 and the number of the re-analyzed LMCs at day 180, is practically equal to 1 in both cases. These results indicate that SLS-MCs and SKL-MCs generated using the optimized protocol display stability profiles over time, comparable to those reported in the previous studies by our research group.[10] These data suggest that the fundamental intermolecular interactions leading to the formation of the lignin microcapsules remain eventually unaffected by the change of conditions used for generating LMCs, thus pointing to a noteworthy robustness of the underlying principles of LMC formation.

Overall, these data confirm the long shelf life of SLS-MCs and SKL-MCs in aqueous, salt-free solutions at pH 7. Storage of LMCs in deionized water is, however, unrealistic with respect to any application scenario. Therefore, the stability in conditions similar to those in intended uses of SLS-MCs, as well as SKL-MCs, especially as carrier systems in industrial, pharmaceutical, and biomedical applications was tested and compared.

Stimuli-Triggered Disassembly of SLS-MCs. *Assessment of Robustness of LMCs: Temperature- and Pressure-*

DOI: 10.1021/acsomega.8b03510
ACS Omega 2019, 4, 6979−6993

Table 2. Assessment of SLS-MC and SKL-MC Temperature- and Pressure-Dependent Disassembly

		mean Ø (μm)		PDI		number of MCs (10^{12} MCs/mL)		stability index	
entry	conditions	SLS	SKL	SLS	SKL	SLS	SKL	SLS	SKL
1	∼1000 mbar, 7 days at RT	1.26	1.55	0.3	0.5	6.57	7.24	1.00	1.00
2	2026 mbar, 30 min at 121 °C	1.32	1.49	0.4	0.5	6.43	7.31	0.98	1.01
3	∼1000 mbar, 7 days at −20 °C	2.19	1.62	0.4	0.4	0.55	0.60	<0.1	<0.1

Dependent Stability. The possible use of lignin microcapsules in biomedical applications in the form of aqueous suspensions comprises systems susceptible to classical sterilization by autoclaving, or freezing for storage and preservation of LMCs hosting temperature-sensitive actives.

SLS-MC robustness has been tested at standard sterilization conditions, that is, under high temperature and high pressure, using an autoclave set at 121 °C and 2026 mbar for 30 min. Interestingly, autoclaved SLS-MCs display similar statistical quantitative analysis data to their reference sample, evidenced by a stability index practically equal to 1 (Table 2, entries 1 and 2). SLS-MCs are thus stable under standard autoclaving settings as applied in industrial, pharmaceutical, and biomedical applications.

Under classical freezing conditions, that is, −20 °C under atmospheric pressure, SLS-MCs undergo a drastic alteration of the statistical quantitative key numbers when compared to their reference sample. The stability index drops below 0.1, that is, >90% of the SLS-MCs were disassembled (Table 2, entry 3). Given that SLS-MCs were suspended in distilled water for these tests, the almost total disassembly of the SLS-MCs upon freezing can be reasoned in the light of the effect of the ice crystals formed in the aqueous environment and the internal microscopic crystals of the oily phase within the SLS-MCs. While these data represent a limitation in the case of temperature-sensitive encapsulants, these results do point, on the other hand, to interesting potential in applications in which the low temperature-triggered release is desired, for example, in optical controls in packaging applications.

pH-Triggered Disassembly of SLS-MCs. The pH-dependent stability studies of SLS-MCs were carried out in a general screening approach for identifying the conditions of disassembly of the stable "concentrated" SLS-MCs as a function of the pH at the site of interest, allowing eventually for the design of targeted release protocols also via targeted chemical modifications of the lignins before LMC formulation.

Electronic interactions have an important role in the science of intermolecular interactions, particularly those involving aromatic rings leading to interactions between the aromatic moieties themselves and between both positively and negatively charged groups and aromatic systems.[39] In addition, coulombic forces can make relevant contributions to stability or disassembly of macromolecular and aggregated structures[40,41] and thus, by analogy, to the stability or cleavage of the SLMC shell structures.

Electrostatic forces are in general strong and have a long range, and they often dominate the properties of supermolecular assemblies. Thus, a pH-triggered disassembly of SLS-MC shell structures can be reasoned in the light of the electrostatic interactions of the system.

SLS contains two types of ionizable groups, that is, sulfonates (pK_a ∼2) and phenolic groups (pK_a ∼10).[24] Therefore, from pH 1 to 2, the SLS moieties are mainly protonated leading to a neutral net charge, which is expected to be distributed throughout the SLS-MC shell. In this context, a possible explanation for the cleavage of more than 90% of the SLS-MCs at these pH values (Table 3, entries 1 and 2 and Figure 2) is the ion−dipole, that is, "cation−π",[42] interactions arising from the electrostatic interactions between the cations, here, H^+ and K^+, and the lignin-inherent π systems of the aromatic groups. These "cation−π" interactions will favor an extended conformation in the extremes hence disassembly rather than a compact structure of the SLS-MC shell.

On the other hand, in the pH range of 3 to 6, the synergistic effect of the "cation−π" interactions, here, mainly between the sodium and the π systems of the aromatic groups, and the intramolecular electrostatic repulsion resulting from the deprotonation of the sulfonate groups in SLS will favor once more an extended conformation, or disassembly, rather than a compact structure of the SLS-MC shell. Overall, the essentially complete disassembly of SLS-MCs, that is, more than 90% in the pH range of 1 to 6, demonstrates the strong detrimental effect of the electrostatic interactions on SLS-MC stability (Figure 2 and Table 3, entries 1 to 6) and underlines the importance of functional electronic interactions between the aromatic moieties for LMC stability.

Based on these observations, a similar behavior of the SLS-based LMCs was expected at alkaline pH. Under stronger alkaline conditions, in addition to the sulfonate groups (pK_a ∼2), the phenolic OH (pK_a ∼10) are also expected to be dissociated, displaying a negative net charge, which is expected to be distributed throughout the SLS-MC shell. Consequently, the intramolecular electrostatic repulsions in combination with the previously reasoned destabilizing "metal cation−π" interactions should favor LMC disassembly. With respect to the strong detrimental effect observed in the acidic environments, however, an increasing stability profile alongside the pH is observed under alkaline conditions (Table 3, entries 8 to 14 and Figure 2A). This increased stability profile of SLS-MCs can be reasoned in light of the increasing concentration of the hydroxide OH^-, which results in increasing ionic interactions overcoming the disassembling cation−π interactions, that is, between Na^+ and the π systems of the aromatic groups.

The differences in the detrimental effects of acidic or alkaline buffer systems on the stability of SLS-MCs may, however, be also reasoned on the basis of a probable stabilizing or destabilizing effect of the ions themselves that characterize the used buffer systems, here, chloride, phosphate, and carbonate anions. A relative increasing proportion of phosphate and/or carbonate anions with respect to the overall ionic contents is observed alongside the seemingly stability-enhancing increase of pH (Table 3, entries 8 to 14). Additional hints at a strong influence of salts in general and specific ion species in particular are visible from the stability tests at pH 7: at neutral pH, a 5-fold increase in molarity of the same buffer system from 0.02 to 0.1 M, corresponding to an increase in salinity from 2.6 to 12.9 ppt, leads to a doubling of the loss of SLS-MCs with respect to the reference sample in deionized water

DOI: 10.1021/acsomega.8b03510
ACS Omega 2019, 4, 6979−6993

Table 3. Assessment of the pH-Dependent Disassembly of SLS-MCs and SKL-MCs under Various Conditions after 48 h

								mean Ø (μm)		PDI		number of MCs (10^{12} MCs/mL)		stability index	
entry	buffer system	pH	salinity (ppt)	chaotropic [mM]	chaotropic (%)	kosmotropic [mM]	kosmotropic (%)	SLS	SKL	SLS	SKL	SLS	SKL	SLS	SKL
1	KCl/HCl	1	4.8	K^+ [29.0], H^+ [100.0], Cl^- [100.0]	100									<0.10	<0.10
2	KCl/HCl	2	5.8	K^+ [56.8], H^+ [10.0], Cl^- [100.0]	100									<0.10	<0.10
3	CH_3COOH/CH_3COONa	3	6.0	Na^+[1.8], H^+ [1.0]	61	CH_3COO^- [1.8]	39							<0.10	<0.10
4	CH_3COOH/CH_3COONa	4	6.3	Na^+ [1.5], H^+ [0.1]	52	CH_3COO^- [1.5]	48							<0.10	<0.10
5	CH_3COOH/CH_3COONa	5	7.5	Na^+ [642.0], H^+ [0.01]	50	CH_3COO^- [642.0]	50							<0.10	<0.10
6	CH_3COOH/CH_3COONa	6	8.1	Na^+ [948.0]	50	CH_3COO^- [948.0]	50							<0.10	<0.10
7	H_2O (reference)	~7						1.26	1.55	0.3	0.5	6.57	7.24	1.00	1.00
8	NaH_2PO_4/Na_2HPO_4	7	12.9	Na^+ [139.0], $H_2PO_4^-$ [61.0]	84	HPO_4^{2-} [39.0]	16	2.00	1.58	0.2	0.4	0.66	1.23	0.10	0.17
9	NaH_2PO_4/Na_2HPO_4	7	2.6	Na^+ [27.8], $H_2PO_4^-$ [12.2]	84	HPO_4^{2-} [7.8]	16	1.45	1.74	0.5	0.5	4.01	4.34	0.61	0.60
10	NaH_2PO_4/Na_2HPO_4	8	12.1	Na^+ [105.3], $H_2PO_4^-$ [94.7]	97	HPO_4^{2-} [5.3]	3	1.90	1.57	0.4	0.5	1.84	2.68	0.28	0.37
11	$NaHCO_3/Na_2CO_3$	9	8.6	Na^+ [110.0], HCO_3^-[90.0]	95	CO_3^{2-} [10.0]	5	2.55	1.45	0.6	0.4	1.91	2.90	0.29	0.40
12	$NaHCO_3/Na_2CO_3$	10	9.5	Na^+ [150.0], HCO_3^-[50.0]	80	CO_3^{2-} [50.0]	20	1.53	1.74	0.5	0.7	2.44	3.05	0.37	0.42
13	$NaHCO_3/Na_2CO_3$	11	10.4	Na^+ [190.0], HCO_3^-[10.0]	70	CO_3^{2-} [90.0]	30	1.30	1.36	0.4	0.3	5.06	3.33	0.77	0.46
14	Na_2HPO_4/Na_3PO_4	12	9.1	Na^+ [100.0]	50	HPO_4^{2-} [50.0], PO_4^{3-} [50.0]	50	1.32	1.38	0.4	0.5	5.65	3.19	0.86	0.44

DOI: 10.1021/acsomega.8b03510
ACS Omega 2019, 4, 6979−6993

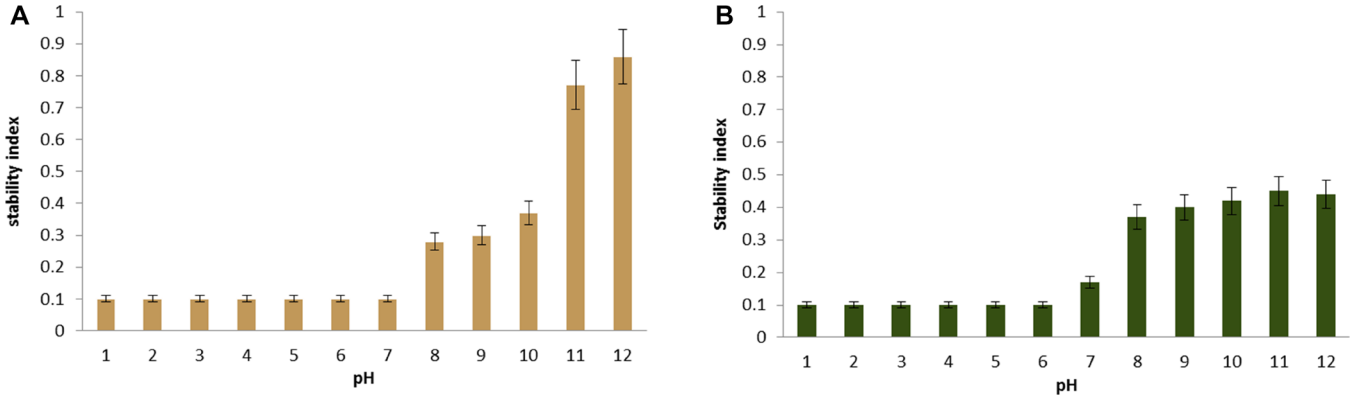

Figure 2. pH-dependent disassembly of (A) SLS-MCs and (B) SKL-MCs.

(Table 3, entries 7 to 9). Therefore, the strong disassembly of SLS-MCs observed at pH 7 in the buffer system at 0.1 M can be reasoned in the light of the detrimental effect of the salinity (Figure 2).

In addition to the decreasing number of SLS-MCs observed in the pH-dependent stability screening, it is generally observed that the remaining SLS-MCs display drastically altered statistical quantitative characteristics with respect to the reference sample. At pH 9, >70% of the SLS-MCs were lost, and the remaining SLS-MCs displayed a practically doubled mean size as well as an increased PDI with respect to the values of these statistical quantitative characteristics in the reference sample (Table 3, entries 7 and 11). Based on these results, the mechanism of SLS-MC disassembly can be reasoned by the following three hypotheses.

Given that in the different pH conditions, the relative net charge is expected to be distributed throughout the shell, in a first approach, the mechanism of SLS-MC disassembly can be explained through a swelling/bursting process, meaning that the different layers of the shell disintegrate by detaching from each other due to the electrostatic repulsions in a centrifugal progressive movement. A second hypothesis is the ripening process, meaning that two or more small SLS-MCs merge together to form one big SLS-MC. An alternative hypothesis is that the swelling/bursting and the ripening processes occur simultaneously (Figure 3).

UV−vis analyses on representative samples in which the remaining LMCs display drastically altered statistical quantitative characteristics allowed for clarifying the nature of capsule alteration (Table 4). As reported in Table 4, columns 2 and 3, in the presence of salts, more than 50% of the SLS-MCs disassembled, and the masses of SLS increased considerably with respect to the reference (changed by 180 and 91 μg vs 9 μg in the reference), suggesting a swelling/bursting process. On the contrary, when surfactants are present (Table 4, columns 4 and 5), ∼50% of the SLS-MCs are disassembled, and the masses of SLS are comparable to the reference (changed by 5 and 11 μg vs 9 μg in the reference), indicating the occurrence of a ripening process. Overall, independent of the pH effect, in surfactant solutions (3-(*N*-morpholino)-propanesulfonic acid (MOPS) and 4-(2-hydroxyethyl)-1-piperazine ethane sulfonic acid (HEPES)), LMCs undergo ripening, whereas in nonsurfactant salt solutions they just swell and burst.

Assessment of Salinity-Dependent Disassembly of SLS-MCs. Electronic interactions between aromatic moieties in organic molecules are strongly dependent, in terms of their

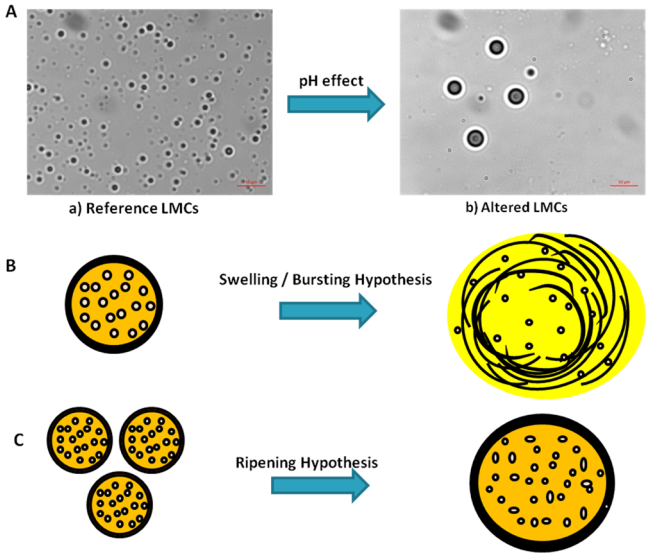

Figure 3. (A) Effect on SLS-MCs at pH 9; (B) swelling/bursting hypothesis; and (C) ripening hypothesis.

effectiveness, on the surrounding conditions set by the solvent and other potential ingredients and additives, like salts or surfactants. With respect to a discussion of LMC stability, these facts are especially important and worth studying given that: (i) early studies on lignin reactivity already indicated that hydrogen bond formation and other secondary valences strongly affect the solubility and colloidal behavior as well as reactivity and general rheological behavior of lignins[16,19,23,43] and (ii) the generation of the LMC shell structure represents a case in which the intrinsic stacking propensities of lignin and its hydrophobic interactions play a key role.[10]

Consequently, kosmotropic and chaotropic agents, classifiable according to the Hofmeister theories[40,44−48] and ordered in the Hofmeister series,[44,49] are expected to affect the LMC shell stability. Chaotropic species should destabilize interactions, whereas kosmotropic agents are expected to have stabilizing effects; mechanistically, this means that ion−dipole interactions between ions of the salts and lignin-inherent dipoles within the aromatic moieties are more determining of the fate of the LMCs than interactions between protons and these lignin-inherent dipoles.[50] Usually, the salt concentration at which specificity shows up is moderately high, for example, above 10−100 mM.[47,51]

DOI: 10.1021/acsomega.8b03510
ACS Omega 2019, 4, 6979−6993

Table 4. Combined Microscopy Imaging and UV−Vis Analysis Data of LMCs Subjected to Various Conditions for 48 h[a]

LMCs	1	2	3	4	5
SLS-MCs	H_2O	$NaHCO_3/CH_3COONa$ (pH 9, 8.6 ppt)	Na_2HPO_4/Na_3PO_4 (pH 12, 9.1 ppt)	MOPS (pH 7, 21 ppt)	HEPES (pH 7, 21 ppt)
	mean Ø: 2.51	mean Ø: 3.18	mean Ø: 4.01	mean Ø: 3.48	mean Ø: 3.80
	yield[b]: 0.197	yield: 44%	yield: 44%	yield: 56%	yield: 47%
	vol. filtrate: 1.15	vol. filtrate: 1.00	vol. filtrate: 1.20	vol. filtrate: 1.08	vol. filtrate:
	concentration: 0.008	concentration: 0.180	concentration: 0.076	concentration: 0.005	concentration: 0.010
	mass: 0.009	mass: 0.180	mass: 0.091	mass: 0.005	mass: 0.011
SKL-MCs	H_2O	NaH_2PO_4/Na_2HPO_4 (pH 7, 2.6 ppt)	NaCl (pH 7, 9 ppt)	$NaHCO_3/Na_2CO_3$ (pH 10, 9.5 ppt)	
	mean Ø: 0.85	mean Ø: 1.03	mean Ø: 0.87	mean Ø: 1.74	
	yield[b]: 0.628	yield: 81%	yield: 38%	yield: 25%	
	vol. filtrate: 1.05	vol. filtrate: 1.20	vol. filtrate: 1.10	vol. filtrate: 1.15	
	concentration: 0.007	concentration: 0.008	concentration: 0.129	concentration: 0.175	
	mass: 0.007	mass: 0.009	mass: 0.142	mass: 0.201	

[a]Mean Ø in μm; volume of filtrate in mL; concentration in mg/mL; mass in mg. [b]Yield in 10^{12} MCs/mL.

With respect to their potential industrial, pharmaceutical, and biomedical applications, a connection between the Hofmeister series and the stability of polyphenol-based nanostructures is established for the first time; that is, the effects of physiologically meaningful ions on LMC stability have been explicitly assessed. Particular attention has been paid to the following kosmotropic anionic and cationic series: $PO_4^{3-} < CO_3^{2-} < SO_4^{2-} < CH_3COO^- < HPO_4^{2-} < Cl^- < H_2PO_4^- < HCO_3^-$, and $Mg^{2+} < Ca^{2+} < H^+ < Na^+ < K^+$, respectively. Obviously, the chaotropic character follows the opposite direction. The results are summarized in Table 6 and need to be seen in connection with the results presented in Table 4 as discussed in the following paragraphs.

Similar statistical quantitative characteristics of SLS-MCs were observed in both deionized H_2O and aqueous Na_2HPO_4 solutions at pH 7 and a salinity of 10 ppt (Table 5, entry 14). In contrast, 2 and 33% of the SLS-MCs were disassembled in aqueous PBS and NaCl solutions at pH 7 and a salinity of ∼10 and 5 ppt, respectively (Table 5, entries 3 and 10). These results underline the applicability of the Hofmeister series for predictions regarding the SLS-MC stability: Phosphate ions as strong kosmotropic agents have a stabilizing effect on SLS-MCs. Chloride anions known as borderline kosmotropic/chaotropic agent, on the other hand, are expected to be more detrimental rather than beneficial. In the case of PBS, the phosphate anion as a strong kosmotropic agent compensates for the deleterious effects of additionally present relatively chaotropic species, here, chloride. This compensatory effect is confirmed by the increasing stability profile of SLS-MCs alongside the increasing proportion of phosphate and/or carbonate in alkaline environments (Table 5, entries 10 to 14).

At neutral pH, 30, 55, and 60% of the SLS-MCs were disassembled after 48 h in aqueous NaCl solutions at 5, 9, and 15 ppt, respectively (Table 5, entries 3, 7, and 18). These results underline the deleterious effect of a high chaotropic content, here, presented by both sodium and chloride ions.

The phenomenon of decreased stability at increasing salinity, observed for aqueous NaCl solutions (Table 5, entries, 3, 7, and 18) is generally also seen in buffer systems containing both chaotropic and kosmotropic agents. One example is the phosphate buffer system containing 84% chaotropic agents, sodium, and dihydrogen phosphate ions and only 16% moderately kosmotropic agent, that is, hydrogen phosphate. As reported in Table 6, entries 2 and 17, 40 and 90% of the SLS-MCs were disassembled in the same type of buffer system by simply augmenting the buffering capacity from 0.02 to 0.1 M, corresponding to an increase in salinity from 2.6 to 12.9 ppt.

More than 90% of the SLS-MCs were disassembled at neutral pH in 0.09 M solutions of $CaCl_2$ and $MgSO_4$ at 10 ppt salinity (Table 5, entries 12 and 13). This is most probably due to the complexation capacity of the dications, that is, Ca^{2+} and Mg^{2+} cations, which induced the disassembly of the SLS-MC shell.

As indicated above, LMC-stability is pH-dependent. Using buffer salts for controlling the pH does, however, also introduce chaotropic and kosmotropic elements into the LMC solution: at different pH values, that is, pH 1 and 7 (Table 5, entries 4 and 11), >90 and ∼70 of the SLS-MCs were disassembled in aqueous KCl solutions at salinities of 4.8 and 10 ppt, respectively. These results indicate that in acidic environments, the chaotropic potential is more effective even at relatively low salinity. The reinforcement of the chaotropic potential by the acidic environment is also seen in buffer systems with the same proportion of both chaotropic and kosmotropic agents.

Overall, except in the case of the kosmotropic dicationic agents, the analytical data summarized in Table 5 are by and large in line with expected cumulative disassociating effects of chaotropic agents and the compensatory effect of the kosmotropic agents, each amplified or tempered by additional pH-related factors.[49,52,53]

Effect of Physiologically Relevant Organic Molecules on the Stability of SLS-MCs. The effects of physiologically relevant organic molecules, that is, proteins and sugars, on the stability of SLS-MCs have been also tested in light of their potential use as carrier systems in pharmaceutical and biomedical applications. Two bovine serum albumin (BSA) solutions (6% w/v) in phosphate (pH 8) and acetate buffer (pH 6) were labelled PBM-1 (physiological background mixture) and PBM-2, respectively.

Portions of the SLS-MCs (25 and ∼40%) were disassembled in PBM-1 (pH 8) and PBM-2 (pH 6), respectively (Table 6, entries 3 and 4). This can be rationalized on the basis of the disassembling effect of the acidic environment in the case of

DOI: 10.1021/acsomega.8b03510
ACS Omega 2019, 4, 6979−6993

Table 5. Assessment of the Salinity-Dependent Disassembly of SLS-MCs and SKL-MCs Subjected to Various Conditions for 48 h

									mean Ø (μm)		PDI		number of MCs (10^{12} MCs/m-L)		stability index	
entry	medium	salinity (ppt)	pH	molarity (mM)	chaotropic [mM]	chaotropic (%)	kosmotropic [mM]	kosmotropic (%)	SLS	SKL	SLS	SKL	SLS	SKL	SLS	SKL
1	H_2O (reference)		~7						1.26	1.55	0.3	0.5	6.57	7.24	1.00	1.00
2	NaH_2PO_4/Na_2HPO_4	2.6	7	20.0	Na^+ [27.8], $H_2PO_4^-$ [12.2]	84	HPO_4^{2-} [7.8]	16	1.45	1.74	0.5	0.5	4.03	4.36	0.61	0.60
3	NaCl	5	~7	85.6	Na^+ [85.6], Cl^- [85.6]	100			1.38	1.55	0.3	0.4	4.40	5.14	0.67	0.71
4	KCl/HCl	4.8	1	100.0	H^+ [100.0], K^+ [29.0], Cl^- [100.0]	100									<0.10	<0.10
5	CH_3COOH/CH_3COONa	8.1	6	100.0	Na^+ [94.8]	50	CH_3COO^- [94.8]	50							<0.10	<0.10
6	$NaHCO_3/Na_2CO_3$	8.6	9	100.0	Na^+ [100.0], HCO_3^- [90.0]	95	CO_3^{2-} [10.0]	5	2.55	1.45	0.6	0.4	0.76	2.23	0.29	0.40
7	NaCl	9	~7	154.1	Na^+ [154.1], Cl^- [154.1]	100			1.60	1.80	0.4	0.4	2.95	4.46	0.45	0.62
8	Na_2HPO_4/Na_3PO_4	9.1	12	100.0	Na^+ [100.0]	50	HPO_4^{2-} [50.0], PO_4^{3-} [50.0]	50	2.32	1.38	0.4	0.5	2.72	1.86	0.86	0.44
9	$NaHCO_3/Na_2CO_3$	9.5	10	100.0	Na^+ [150.0], HCO_3^- [50.0]	80	CO_3^{2-} [50.0]	20	1.53	1.74	0.5	0.3	1.18	2.16	0.37	0.42
10	PBS	9.9	~7	100.0	Na^+ [157.3], K^+ [4.4], Cl^- [139.7], $H_2PO_4^-$ [1.8]	97	HPO_4^{2-} [10.1]	3	1.29	1.40	0.3	0.5	6.49	6.75	0.98	0.93
11	KCl	10	~7	134.1	K^+ [134.1], Cl^- [134.1]	100			1.49	1.36	0.4	0.4	1.75	1.57	0.26	0.22
12	$CaCl_2$	10	~7	90.1	Cl^- [180.2]	67	Ca^{2+} [90.1]	33							<0.10	<0.10
13	$MgSO_4$	10	~7	80.1			Mg^{2+} [80.1], SO_4^{2-} [80.1]	100							<0.10	<0.10
14	Na_2HPO_4	10	7	70.4	Na^+ [140.9]	67	HPO_4^{2-} [70.4]	33	1.35	1.60	0.5	0.5	6.24	7.23	0.95	1.00
15	$NaHCO_3/Na_2CO_3$	10.4	11	100.0	Na^+ [190.0], HCO_3^- [10.0]	70	CO_3^{2-} [90.0]	30	1.30	1.36	0.4	0.3	2.43	2.47	0.77	0.46
16	NaH_2PO_4/Na_2HPO_4	12.1	8	100.0	Na^+ [105.3], $H_2PO_4^-$ [94.70]	97	HPO_4^{2-} [5.3]	3	1.90	1.57	0.4	0.5	0.96	2.01	0.28	0.37
17	NaH_2PO_4/Na_2HPO_4	12.9	7	100.0	Na^+ [139.0], $H_2PO_4^-$ [61.0]	84	HPO_4^{2-} [39.00]	16	2.00	1.58	0.2	0.4	0.31	0.94	0.10	0.17
18	NaCl	15	~7	256.9	Na^+ [256.9], Cl^- [256.9]	100			1.59	1.05	0.4	0.6	2.43	3.26	0.37	0.45

DOI: 10.1021/acsomega.8b03510
ACS Omega 2019, 4, 6979−6993

Table 6. Assessment of the Effect of Organic Molecules on the Disassembly of SLS-MCs and SKL-MCs Subjected to Various Conditions for 48 h[a]

				mean Ø (μm)		PDI		number of MCs (10^{12} MCs/mL)		stability index	
entry	organic molecule solution	pH	conc (% w/v)	SLS	SKL	SLS	SKL	SLS	SKL	SLS	SKL
1	H_2O (reference)	~7		1.26	1.55	0.3	0.5	6.57	7.24	1.00	1.00
2	BSA	~8	6	1.31	1.31	0.4	0.4	5.97	6.83	0.90	0.94
3	PBM-1	~8	6	1.32	1.61	0.4	0.5	4.77	6.13	0.75	0.86
4	PBM-2	~6	6	1.34	1.37	0.4	0.5	3.77	2.58	0.60	0.36
5	glucose	~7	5	1.22	1.51	0.4	0.4	5.26	6.63	0.80	0.92

[a]BSA, bovine serum albumin; PBM-1, physiological background mixture-1 in phosphate buffer system; PBM-2, physiological background mixture-2 in acetate buffer system.

Table 7. Assessment of the Effect of Surfactant on the Disassembly of SLS-MCs and SKL-MCs Subjected to Various Conditions for 48 h[a]

					mean Ø (μm)		PDI		number of MCs (10^{12} MCs/mL)		stability index	
entry	surfactant	pH	incubation time (h)	salinity (ppt)	SLS	SKL	SLS	SKL	SLS	SKL	SLS	SKL
1	H_2O (reference)	~7			1.26	1.55	0.3	0.5	6.57	7.24	1.00	1.00
2	HLSA[a]	2	8	45	3.41	1.29	2.2	0.6	0.65	1.42	0.09	0.20
3	HLSA	2	24	45	1.92	1.57	1.2	0.6	0.71	0.85	0.10	0.12
4	HLSA	2	48	45	2.33	1.18	1.3	0.6	0.83	1.16	0.12	0.16
5	SDS	~7	48	29	1.69	1.31	0.5	0.5	4.59	3.84	0.70	0.53
6	AE-25[b]	7	8		1.27	1.32	0.5	0.6	4.17	4.85	0.63	0.67
7	AE-25	7	24		1.41	1.54	0.5	0.5	2.45	3.90	0.37	0.54
8	AE-25	7	48		1.34	1.22	0.3	0.6	2.32	3.49	0.35	0.48
9	MOPS	~7	48	21	1.93	1.52	0.5	0.5	3.28	5.44	0.50	0.75
10	AO[c]	8	8	54	1.73	1.52	0.5	0.6	1.97	7.26	0.30	1.00
11	AO	8	24	54	1.66	1.54	0.6	0.4	2.01	6.88	0.31	0.95
12	AO	8	48	54	1.79	1.53	0.6	0.5	2.15	6.65	0.33	0.92

[a]HLSA, high linear alkylbenzene sulfonate; AE-25, alcohol ethoxylate; AO, amine oxide.

PBM-2 and on the basis of the kosmotropic effect of the phosphate anions in the case of PBM-1.

A 6% w/v BSA solution in distilled H_2O was tested for the "protein effect" alone; the concentration corresponds to the physiological concentration of the overall protein content in blood. In such a solution, no significant capsule disassembly occurred, demonstrating that pure albumin does not significantly affect SLS-MC stability (Table 6, entries 1 and 2).

In a 5% w/v aqueous glucose solution, corresponding to the standard glucose concentration for eventual intravenous administrations, ~20% of the SLS-MCs were disassembled (Table 6, entry 5); this demonstrates that glucose has slightly detrimental effects on SLS-MC shell stability.

Effect of Surfactants on the Stability of SLS-MCs. As intuitively expectable, the effect of surfactants on the SLS-MC stability also has to be assessed in connection with salinity- and pH-effects in light of potential applications of LMCs, here, especially in home and personal care products. By definition, surfactants are compounds that lower the surface or interfacial tension between two liquids, between a gas and a liquid, or between a liquid and a solid.[54,55] The assessment of such effects of surfactants on SLS-MC stability was realized in 5% v/v aqueous solutions of different types of industrially used surfactants, represented by an alcohol ethoxylate (AE-25) as a nonionic surfactant, an amine oxide (AO) as an amphoteric surfactant, and a high linear alkylbenzene sulfonate (HLSA) as a synthetic anionic surfactant. Sodium dodecyl sulfonate (SDS) and 3-(*N*-morpholino)propanesulfonic acid (MOPS) were used as buffer systems commonly used in biological contexts.

In aqueous solution of AE-25 at neutral pH, ~60% of the SLS-MCs were disassembled (Table 7, entries 6 to 8). These results indicate that surfactants significantly affect SLS-MC stability, whose effect may be eventually amplified by pH and salinity.

Aqueous amphoteric surfactants have been tested by using AO at pH 8 and a salinity of 54 ppt. As results have shown, ~70% of the SLS-MCs were disassembled (Table 7, entries 10 to 12), underlining the high-salinity driven relative amplification of the detrimental effect of surfactants on SLS-MCs. In addition, the electrostatic repulsions between the sulfonates present in the SLS-MC shell and the AO zwitterions contribute also to the disassembling effect.

HLAS has been used as an exemplary alkylbenzene sulfonate surfactant. Aqueous HLAS solution at pH 2 and a salinity of 45 ppt causes ~90% of the SLS-MCs to disassemble (Table 7, entries 2 to 4).

In aqueous surfactant solutions of SDS (29 ppt) and MOPS (21 ppt), 40 and 30% of the SLS-MCs were disassembled, respectively (Table 7, entries 5 and 9). In comparison to a nonsurfactant aqueous solution at relatively low salinity, that is, NaCl (15 ppt), in which 60% of the SLS-MCs were disassembled (Table 5, entry 18), MOPS and SDS have thus only moderate destructive effects on SLS-MCs even at relatively high salinities.

Assessment of the Stability of SLS-MCs in Organic Solvents. The stability profile of SLS-MCs in organic solvents

DOI: 10.1021/acsomega.8b03510
ACS Omega 2019, 4, 6979−6993

Table 8. Assessment of the Disassembly of SLS-MCs and SKL-MCs in Organic Solvents by Dialysis for 24 h

		mean Ø (μm)		PDI		number of LMCs (10^{12} LMCs/mL)		stability index		identified oil component[a]			
entry	organic solvent	SLS	SKL	SLS	SKL	SLS	SKL	SLS	SKL	A	B	C	D
1	reference	1.26	1.55	0.3	0.5	6.57	7.24	1.00	1.00				
2	toluene	1.23	1.24	0.4	0.4	2.30	2.90	0.35	0.39	8.55	1.10	58.64	6.46
3	hexane	1.40	1.35	0.6	0.6	4.95	3.67	0.56	0.51	10.85	1.13	61.83	7.56
4	ethanol									2.45	5.96	26.32	13.47

[a]Area % of the GC−MS data obtained from the oily phase and the concentrated organic solvents from the dialysis: (A) palmitic acid, (B) linoleic acid, (C) oleic acid, and (D) stearic acid.

has been assessed in light of potential applications in organic synthesis, for example as a catalyst housing. Aqueous SLS-MC suspensions were dialyzed against apolar aliphatic, nonpolar aromatic, and polar protic organic solvents for 24 h. This screening aimed to evaluate the effect of osmotic stress on the SLS-MC stability.

As reported in Table 8, ∼60 and 50% of the SLS-MCs were disassembled in toluene and hexane, respectively. A possible explanation for the cleavage of SLS-MCs is the lysis of the SLS-MC shells due to osmotic effects. This is corroborated by the presence of elements of the oily phase in the organic solvents (Table 8, entries 2 and 3). The representative fatty acid components of olive oil revealed by the GC−MS analysis demonstrate the cleavage of the LMC shell structures.

Hofmeister effects occur universally in aqueous electrolyte systems; however, some studies demonstrate the occurrence of specific ion effects on the activity of enzymes also in non-aqueous media.[56] In addition, the existence of chaotropic organic solvents, like ethanol, has been demonstrated.[57] The complete disassembly of SLS-MCs in organic solvents can thus be attributed to the synergistic action of the no osmosis/poor osmosis and chaotropic potential of ethanol (Table 8, entry 4).

Stimuli-Triggered Disassembly of SKL-MCs. At present, SKL is one of the most cost-effective available lignins in industrial quantities.[22] Therefore, development of materials based on SKL should be beneficial for the future sustainable society and add value to a renewable resource. In this respect, a study of stimuli-triggered disassembly of SKL-MCs was carried out in light of their potential use as carrier systems for industrial applications as a potential alternative to SLS-MCs previously discussed.

Assessment of Temperature- and Pressure-Dependent Stability of SKL-MCs. Autoclaved SKL-MCs, like autoclaved SLS-MCs, display similar statistical quantitative analytical data in comparison to their reference samples (Table 2, entries 1 and 2), demonstrating their suitability for applications in which sterilization processes might be required.

Similar to frozen SLS-MCs, the statistical quantitative characteristics of the frozen SKL-MCs are altered significantly when compared to the reference sample. Approximately 90% of SKL-MCs disassembled after freezing and the remaining SKL-MCs display practically the double of the mean size with a high PDI with respect to the reference sample (Table 2, entry 3).

Assessment of pH-Dependent Disassembly of SKL-MCs. In acidic environments, that is, a pH range of 1 to 6, more than 90% of the SKL-MCs were disassembled (Table 3, entries 1 to 6). This complete cleavage of the SKL-MCs is essentially due to the "cation−π" interactions, as discussed in the case of SLS-MCs.

However, at alkaline pH, that is, a pH range from 8 to 12, SKL-MCs and SLS-MCs display different stability profiles. In the alkaline buffer systems, ∼60% of the SKL-MCs were disassembled regardless of the molarity or the salinity, whereas SLS-MCs display an increasing stability profile alongside the pH (Table 3, entries 10 to 14). This can be rationalized on the basis of their different structure and the pK_a difference, that is, pK_a ranges from 1.8 to 6.9[58] and from ∼6 to ∼11[16,23,59] for SLS and SKL, respectively.

In the considered alkaline pH range of 8 to 10, the acid groups are expected to be dissociated by and large, displaying a negative net charge on the SKL-MC shell. Consequently, intermolecular electrostatic repulsions should stabilize the SKL-MC. On the contrary, at low pH values, the lower electrostatic repulsion would favor the ripening processes. Furthermore, ionic interactions, that is, Na^+ and $RCOO^-$ from the deprotonated SKL as well as Na^+ and OH^-, are more favored than the disassembling cation−π interactions, that is, Na^+ and π systems of the aromatic groups present in SKL. In addition, the only moderate detrimental effect of the alkaline buffer systems on SKL-MCs may be also due to a stabilizing effect of phosphate and carbonate anions.

Assessment of Salinity-Dependent Disassembly of SKL-MCs. As summarized in Table 4, in the range of the established average error, the results of the salinity-dependent disassembly of SKL-MCs are comparable to the general trend of the salinity-dependent disassembly of SLS-MCs.

Effect of Organic Molecules on the Stability of SKL-MCs. Comparable statistical quantitative analytical data were observed in both SKL-MC and SLS-MC stability screening in organic molecules, that is, perfectly stable in BSA and glucose and moderately stable in PBM-1 and PBM-2. Data are given in Table 6.

Effect of Surfactants on the Stability of SKL-MCs. The effect of surfactants on the stability of SKL-MCs has been determined in the same manner as already discussed above for the case of SLS-MCs. As reported in Table 7, aqueous nonionic surfactants, such as AE-25, have a moderate detrimental effect in both SLS-MCs and SKL-MCs, that is, ∼50% of the SKL-MCs and ∼60% of the SLS-MCs were disassembled.

However, SKL-MCs display a different stability profile in aqueous AO at pH 8 and 54 ppt salinity: under these conditions, they are not significantly affected, whereas under the same conditions, ∼70% of the SLS-MCs were disassembled (Table 7, entries 10 to 12). This difference is due to the electrostatic repulsions between the sulfonates and the AO zwitterions resulting in the strong disassembling effect on the SLS-MC shell.

In aqueous HLAS solution at pH 2 and a salinity of 45 ppt, ∼90% of both the SKL-MCs and SLS-MCs were disassembled

DOI: 10.1021/acsomega.8b03510
ACS Omega 2019, 4, 6979−6993

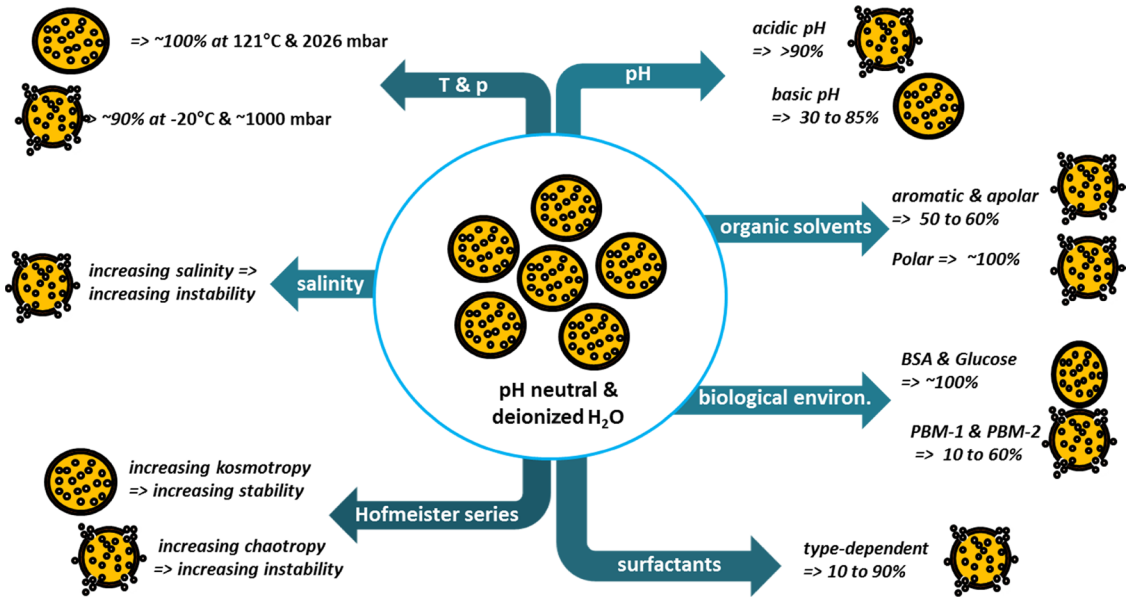

Figure 4. Overview demonstrating LMC stabilities under various conditions.

(Table 7, entries 2 to 4), demonstrating that the deleterious effect of the strongly acidic pH and high salinity on SLS-MC stability is stronger than any potential stabilizing effect of the considered surfactant.

Assessment of the Disassembly of SKL-MCs in Organic Solvents. As summarized in Table 8, the analytical data of the disassembly of SKL-MCs and SLS-MCs in organic solvents have similar general trends.

CONCLUSIONS

Technical lignins have shown to be excellent matrices for the ultrasound-mediated synthesis of microcapsules for active delivery. Irrespective of the industrial origin, microcapsules can be efficiently synthesized with different stimuli-responsive behaviors. Lignosulfonate microcapsules have been synthesized, and their stability and stimuli-responsive behavior have been studied in comparison with the responsiveness of kraft lignin microcapsules. Strategies for increasing efficiency in the generation of ultrasound-assisted LMCs have been achieved using both softwood lignosulfonate (SLS) and softwood kraft lignin (SKL).

LMCs show excellent stability over time under high temperature and pressure (autoclaving conditions). They also display excellent to very good stability in solutions of physiologically relevant organic molecules, that is, proteins and sugars, which is of crucial relevance in the case of pharmaceutical applications. Stimuli-triggered disassembly can be induced by tuning the pH conditions: they are stable in alkaline conditions (pH 7 to 12) and disassemble under acidic conditions (pH 1 to 6). Lignosulfonate microcapsules show higher stability than the kraft lignin ones at alkaline pH values. The salinity of the medium is a further tool to trigger capsule disassembly and active release. Surfactants also affect significantly LMC stability, whose effect may be eventually amplified by pH and salinity. Figure 4 graphically summarizes the findings of this work.

The generation of the LMC shell structure represents a case in which the intrinsic stacking propensities of lignin and its hydrophobic interactions play a key role.[10] Consequently, when approaching the salinity effect on the stability of LMCs, the chaotropic or kosmotropic nature of the salts employed has to be taken into consideration. Therefore, this paper establishes a connection between the Hofmeister series and stability of polyphenol-based nanostructures. Overall, except in the case of the kosmotropic dicationic agents, the analytical data are by and large in line with the expected cumulative disassociating effect of chaotropic agents and the associating effect of the kosmotropic agents.

The results as a whole indicate differences between SLS-LMCs and SKL-LMCs. These differences are expected from their chemical differences. Chemical characteristics, however, can be efficiently altered by chemically transforming specific functional groups in lignins. Such alterations can be used for altering LMC characteristics, as has been shown by our group in very early studies. The beauty of the simple LMCs generated only on the basis of intermolecular interactions, however, lies in the fact that the lignin is used as it is, omitting additional costs and the environmental burden connected to upstream or concomitant chemical lignin modification. The present study forms the basis for constructing LMCs with specific stability profiles by choosing the most suitable lignin or mixture of lignins.

EXPERIMENTAL SECTION

General Information. Chemicals and solvents were purchased from Sigma-Aldrich or Carlo Erba in appropriate grades and were used without further purification if not stated otherwise. Softwood lignosulfonate (SLS) was obtained from Borregard; softwood kraft lignin (SKL) was obtained from the French Institute of Technology "Forêt Cellulose Bois-construction Ameublement" (FCBA).

Preparation of Aqueous SLS and SKL Solutions. An aqueous SLS solution (0.5% w/v) was freshly prepared by dissolving 100 mg of SLS in 20 mL of distilled H_2O. The pH of the system was adjusted to pH ~12 by adding some drops of aqueous 1 N NaOH. An aqueous SKL solution (0.5% w/v) was prepared for each use by suspending 100 mg of SKL in 20 mL of distilled H_2O. The SKL solution was obtained by adding some drops of aqueous 1 N NaOH, raising the pH of the system to pH ~12.

DOI: 10.1021/acsomega.8b03510
ACS Omega 2019, 4, 6979−6993

Preparation of Starting Emulsion and LMC Generation. The aqueous SLS or SKL solutions (500 μL) were mixed with 500 μL of olive oil. This biphasic system was magnetically stirred for 5 min. Using a Branson digital sonifier (Model 450L, Ultrasonic Corporation) equipped with a 20 kHz Branson probe ending in a sonication tip, the mixture was then ultrasonicated at room temperature (RT) with a power of 160 W (40% amplitude) for 10 min.

Isolation of the LMCs. The isolation of the LMCs from the remaining liquid was realized by centrifugation of the emulsion obtained after sonication at 5000 rpm for 15 min. The lower aqueous phase was removed, and the foamy supernatant consisting of the LMCs was washed as follows to remove residual lignin and oil. "Washing" consisted of re-suspending the LMCs in 1000 μL of distilled H_2O before repeating the centrifugation and phase separation step as previously described. This "washing" was performed at least twice to obtain the "concentrated", that is, densely packed LMCs. The pH of these "concentrated" LMCs was ∼7.

Preparation of Buffer Solutions. Buffers were prepared using appropriate ratios of the salts establishing the buffer systems listed in Table 9.

Table 9. Buffer Systems at Different pH, Salinity, and Molarity Values

entry	buffer system	pH	salinity (ppt)	molarity (M)
1	KCl/HCl	1	4.8	0.1
2	KCl/HCl	2	5.8	0.1
3	CH_3COOH/CH_3COONa	3	6.0	0.1
4	CH_3COOH/CH_3COONa	4	6.3	0.1
5	CH_3COOH/CH_3COONa	5	7.4	0.1
6	CH_3COOH/CH_3COONa	6	8.1	0.1
7	NaH_2PO_4/Na_2HPO_4	7	12.9	0.1
8	NaH_2PO_4/Na_2HPO_4	7	2.6	0.02
9	NaH_2PO_4/Na_2HPO_4	8	12.1	0.1
10	$NaHCO_3/Na_2CO_3$	9	8.6	0.1
11	$NaHCO_3/Na_2CO_3$	10	9.5	0.1
12	$NaHCO_3/Na_2CO_3$	11	10.4	0.1
13	Na_2HPO_4/Na_3PO_4	12	9.1	0.1
14	Na_2HPO_4/Na_3PO_4	12	4.6	0.05

Preparation of Salt Solutions. Aqueous phosphate buffered saline (PBS) solution (0.1 M) was prepared by dissolving 0.800 g of NaCl, 0.020 g of KCl, 0.144 g of Na_2HPO_4, and 0.024 g of KH_2PO_4 in 80.0 mL of distilled H_2O.[38] The pH was adjusted to 7.4 by using 1 N aqueous NaOH before the solution was brought to a final volume of 100 mL.

Aqueous (3-(N-morpholino)propanesulfonic acid (MOPS) solution (0.1 M) was prepared by dissolving 0.523 g of MOPS in 25 mL of distilled H_2O, and the pH was adjusted to 7.4 with 1 N aqueous NaOH.

Aqueous (4-(2-hydroxyethyl)-1-piperazine ethane sulfonic acid (HEPES) solution (0.1 M) was prepared by dissolving 0.596 g of HEPES in 25 mL of distilled H_2O, and the pH was adjusted to 7.4 with 1 N aqueous NaOH.

Aqueous sodium dodecyl sulfate (SDS) solution (0.1 M) was prepared by dissolving 1.442 g of SDS in 50 mL of distilled H_2O. The pH of this solution was ∼7.

Aqueous NaCl solutions at different concentrations were prepared by dissolving 50, 90, and 150 mg of NaCl in 10 mL of distilled H_2O; aqueous NaCl solutions of 0.08, 0.15, and 0.26 M with salinities of 5, 9, and 15 ppt, respectively, were obtained. The pH of these solutions was ∼7.

Aqueous KCl, $CaCl_2$, and $MgSO_4$ solutions at 10 ppt salinity were prepared by dissolving 100 mg of each salt in 10 mL; aqueous KCl, $CaCl_2$, and $MgSO_4$ solutions with concentrations of 0.13, 0.09, and 0.08 M, respectively, were obtained. The pH of these solutions was ∼7.

Preparation of Surfactant Solutions. Aqueous solutions of selected industrial surfactants, that is, alcohol ethoxylate (AE-25), high linear alkylbenzene sulfonate (HLSA), and amine oxide (AO), were prepared at 5% v/v.

Preparation of Aqueous Solutions of Physiologically Relevant Organic Molecules. Aqueous protein solutions were prepared at 6% w/v, that is, bovine serum albumin (BSA) in distilled H_2O at pH ∼8 and mixture enzymes in phosphate and acetate buffer systems at 6% w/v at pH 8 and 6, respectively. These mixture enzymes were labelled PBM-1 (physiological background mixture) and PBM-2. An aqueous glucose solution at pH 7 was prepared at 5% w/v.

Temperature- and Pressure-Triggered Release Screening. The "concentrated" LMCs (10 μL) were dispersed in 990 μL of distilled H_2O in an Eppendorf tube suitable for high temperatures. An aliquot was analyzed via optical microscopy before and after the freezing and the heating processes. The freezing was performed at room pressure (∼1000 mbar) for 1 week, and the heating was performed in an autoclave at 121 °C at 2026 mbar for 30 min.

Screening of LMC Disassembly in Various Aqueous Media. The generated "concentrated" LMCs (10 μL) were dispersed in an Eppendorf tube containing 990 μL of the medium in which the stability of the LMCs was to be determined. LMCs were dispersed homogeneously by gently shaking the system for 2 min. The system was then observed for eventual macroscopic changes in its consistency before it was kept at the various conditions for the indicated times with occasional redispersing of eventually settled LMCs. The system was gently shaken again, and an aliquot was taken and analyzed via optical microscopy as discussed below.

Screening of LMC Disassembly in Organic Solvents Via Dialysis. The "concentrated" LMCs (10 μL) were dispersed in an Eppendorf tube containing 990 μL of distilled H_2O. The dispersion of the LMCs was performed by gently shaking the system for 2 min. Thereafter, the system was transferred into a dialysis bag, and the dialysis bag was placed in a beaker containing either toluene, hexane, or ethanol and left stirring at RT for 24 h. Aliquots of the aqueous phase were analyzed via optical microscopy before and after the dialysis. In addition, aliquots of the toluene, hexane, or ethanol phases were analyzed by gas chromatography coupled to mass spectrometry (GC−MS) after concentration.

Gas Chromatography Coupled to Mass Spectrometry (GC−MS). *Sample Preparation.* Ethyl acetate (∼600 μL) was used to dissolve the concentrated organic solvents, that is, toluene, hexane, and ethanol phases from the dialysis process. In situ silylation of the sample is performed by means of addition of 50 μL of pyridine, followed by addition of 50 μL of *N*,*O*-bis(trimethylsilyl)trifluoroacetamide 15 min before analysis.

Measurement. Analysis was carried out on 5 μL aliquots using a Shimadzu GC−MS QP2010 Ultra equipped with an AOi20 autosampler unit. An SLB-5ms capillary GC column (*L* × I.D. 30 m × 0.32 mm; df, 0.50 μm) was used as the stationary phase, and He was used as the mobile phase at 100

DOI: 10.1021/acsomega.8b03510
ACS Omega 2019, 4, 6979−6993

kPa pressure, 240 °C injection temperature, and 200 °C interface temperature. Program: 50 °C start temperature for 1 min, 10 °C/min heating rate, and 240 °C final temperature for 15 min. Mass analysis was performed after electron ionization using ∼70 eV. Analysis was performed by using Shimadzu GC−MS Solution software (version 2.61).

UV−Vis Analysis. *Sample Preparation.* The generated "concentrated" LMCs (10 μL) was dispersed in an Eppendorf tube containing 990 μL of the medium in which the stability of the LMCs was to be determined. LMCs were dispersed homogeneously by gently shaking the system for 2 min. After the microscopy analysis, the system was filtered out, and the filtrate was used for UV−vis analysis.

Optical Microscopy Analysis and Statistical Analysis. *Sample Preparation.* The generated "concentrated" LMCs (10 μL) was added into 990 μL of distilled H_2O to form a suspension of LMCs. This suspension (5 μL) was transferred onto a microscope carrier glass slide and covered with a coverslip before microscopy analysis. In case the capsules overlap to a large extent, the sample should be further diluted before analysis.

Analysis. A Zeiss Axio Scope A1 microscope was used for the image analysis. All images were obtained with 100× objective lens magnification. For optimizing the use of the 100× lens, a drop of mineral oil was placed on the coverslip before the analysis to function as an optical bridge.

Processing. The pictures from the microscope were processed by using the image analysis software ImageJ in combination with Microsoft Office Excel-based analyses for generating statistical data for the LMC samples. These statistical data are basically the LMC mean diameter, the number of LMCs, the polydispersity index (PDI) of the LMC diameter calculated according to the formula σ/μ (where σ is the standard deviation and μ the mean diameter of the LMCs in the sample under analysis), and the stability index, which is the ratio between the number of LMCs after each experimental conditions and the standard conditions.

The different screenings were performed on the basis of statistical key figures (10 μL "concentrated" LMCs at pH ∼7 in 990 μL distilled H_2O before analysis, RT, and 1 atm unless stated otherwise). Three images were chosen for the software-based ImageJ analysis. Error analysis was performed according to this protocol using 10 different samples. A comparison between manual counting and ImageJ software-based counting has been accomplished, screening different settings in the software. Based on these various evaluations of the quality of the computer-based analysis, an average error of the diameter and the number of MCs per milliliter, 0.06 μm and 0.15×10^{12} LMCs/mL, respectively, were established.

AUTHOR INFORMATION

Corresponding Author

*E-mail: claudia.crestini@unive.it. Tel.: +39 0412348546.

ORCID

Claudia Crestini: 0000-0001-9903-2675

Author Contributions

The manuscript was written through contributions of L.Z., H.L., and C.C. The experimental work was performed by L.Z. The results were interpreted by L.Z., H.L., and C.C. All authors have given approval to the final version of the manuscript.

Notes

The authors declare no competing financial interest.

ACKNOWLEDGMENTS

Borregard and the French Institute of Technology "Forêt Cellulose Bois-construction Ameublement" (FCBA) are gratefully acknowledged for providing softwood lignosulfonate (SLS) and softwood kraft lignin (SKL), respectively.

ABBREVIATIONS

NPs	natural polyphenols
LMCs	lignin microcapsules
SKL	softwood kraft lignin
SKL-MCs	softwood kraft lignin microcapsules
SLS	softwood lignosulfonate
LS-MCs	lignosulfonate microcapsules
RT	room temperature
SDS	sodium dodecyl sulfate
AO	amine oxide
AE	alcohol ethoxylate
HLAS	high linear alkylbenzene sulfonate
PBS	phosphate buffered saline
MOPS	3-(*N*-morpholino)propanesulfonic acid
HEPES	4-(2-hydroxyethyl)-1-piperazine ethane sulfonic acid
BSA	bovine serum albumin
PBM-1	physiological background mixture-1 in phosphate buffer system
PBM-2	physiological background mixture-2 in acetate buffer system
UV−vis	ultraviolet−visible
GC−MS	gas chromatography−mass spectrometry

REFERENCES

(1) Chang, T. M. S. Semipermeable Microcapsules. *Science* **1964**, *146*, 524−525.

(2) Manickam, S.; Ashokkumar, M. *Cavitation: A Novel Energy-Efficient Technique for the Generation of Nanomaterials*; CRC Press, 2014.

(3) Umer, H.; Nigam, H.; Tamboli, A. M.; Nainar, M. S. M. Microencapsulation: Process, Techniques and Applications. *Int. J. Res. Pharm. Biomed. Sci.* **2011**, *2*, 474−481.

(4) Guarda, A.; Rubilar, J. F.; Miltz, J.; Galotto, M. J. The Antimicrobial Activity of Microencapsulated Thymol and Carvacrol. *Int. J. Food Microbiol.* **2011**, *146*, 144−150.

(5) Tsuji, K. Microencapsulation of Pesticides and Their Improved Handling Safety. *J. Microencapsulation* **2001**, *18*, 137−147.

(6) Singh, M. N.; Hemant, K. S. Y.; Ram, M.; Shivakumar, H. G. Microencapsulation: A Promising Technique for Controlled Drug Delivery. *Res. Pharm. Sci.* **2010**, *5*, 65.

(7) Desai, K. G. H.; Jin Park, H. Recent Developments in Microencapsulation of Food Ingredients. *Drying Technol.* **2005**, *23*, 1361−1394.

(8) Zhao, Q.; Han, B.; Wang, Z.; Gao, C.; Peng, C.; Shen, J. Hollow Chitosan-Alginate Multilayer Microcapsules as Drug Delivery Vehicle: Doxorubicin Loading and in Vitro and in Vivo Studies. *Nanomedicine Nanotechnol. Biol. Med.* **2007**, *3*, 63−74.

(9) Broaders, K. E.; Pastine, S. J.; Grandhe, S.; Fréchet, J. M. J. Acid-Degradable Solid-Walled Microcapsules for PH-Responsive Burst-Release Drug Delivery. *Chem. Commun.* **2011**, *47*, 665−667.

(10) Bartzoka, E. D.; Lange, H.; Thiel, K.; Crestini, C. Coordination Complexes and One-Step Assembly of Lignin for Versatile Nanocapsule Engineering. *ACS Sustainable Chem. Eng.* **2016**, *4*, 5194−5203.

DOI: 10.1021/acsomega.8b03510
ACS Omega 2019, 4, 6979−6993

(11) Chen, L.; Subirade, M. Elaboration and Characterization of Soy/Zein Protein Microspheres for Controlled Nutraceutical Delivery. *Biomacromolecules* **2009**, *10*, 3327−3334.
(12) Tomaro-Duchesneau, C.; Saha, S.; Malhotra, M.; Kahouli, I.; Prakash, S. Microencapsulation for the Therapeutic Delivery of Drugs, Live Mammalian and Bacterial Cells, and Other Biopharmaceutics: Current Status and Future Directions. *J. Pharm.* **2013**, *2013*, 103527.
(13) Nazzaro, F.; Orlando, P.; Fratianni, F.; Coppola, R. Microencapsulation in Food Science and Biotechnology. *Curr. Opin. Biotechnol.* **2012**, *23*, 182−186.
(14) Tortora, M.; Cavalieri, F.; Mosesso, P.; Ciaffardini, F.; Melone, F.; Crestini, C. Ultrasound Driven Assembly of Lignin into Microcapsules for Storage and Delivery of Hydrophobic Molecules. *Biomacromolecules* **2014**, *15*, 1634−1643.
(15) Chang, T. M. S. Artificial Cells for Cell and Organ Replacements. *Artif. Organs* **2004**, *28*, 265−270.
(16) Ludwig, C. H.; Sarkanen, K. V. *Lignins: Occurrence, Formation, Structure and Reactions*; Wiley-Interscience, 1971.
(17) Heitner, C.; Dimmel, D.; Schmidt, J. *Lignin and Lignans: Advances in Chemistry*; CRC press, 2016.
(18) Gellerstedt, G.; Henriksson, G. In *Monomers, Polymers and Composites from Renewable Resources;* Belgacem, M.; Gandini, A., Eds; Elsevier: Oxford, United Kingdom, 2008.
(19) Sarkanen, S.; Teller, D. C.; Stevens, C. R.; McCarthy, J. L. Lignin. 20. Associative Interactions between Kraft Lignin Components. *Macromolecules* **1984**, *17*, 2588−2597.
(20) Bartzoka, E. D.; Crestini, C.; Lange, H. *Biomass Derived and Biomass Inspired Polymers in Pharmaceutical Applications*; John Wiley & Sons, Inc, 2015.
(21) Lange, H.; Schiffels, P.; Sette, M.; Sevastyanova, O.; Crestini, C. Fractional Precipitation of Wheat Straw Organosolv Lignin: Macroscopic Properties and Structural Insights. *ACS Sustainable Chem. Eng.* **2016**, *4*, 5136−5151.
(22) Gellerstedt, G. Softwood Kraft Lignin: Raw Material for the Future. *Ind. Crops Prod.* **2015**, *77*, 845−854.
(23) Glasser, W. G.; Sarkanen, S. *Lignin: Properties and Materials*; ACS Publications, 1989.
(24) Sanghi, R.; Singh, V. *Green Chemistry for Environmental Remediation*; John Wiley & Sons, 2012.
(25) Adams, J. W. *Environmental Effects of Applying Lignosulfonate to Roads*; Daishowa chemicals Incorporated, 1988.
(26) Stapanian, M. A.; Shea, D. W. Lignosulfonates: Effects on Plant Growth and Survival and Migration through the Soil Profile. *Int. J. Environ. Stud.* **1986**, *27*, 45−56.
(27) Doudoroff, P.; Katz, M. Critical Review of Literature on the Toxicity of Industrial Wastes and Their Components to Fish: II. the Metals, as Salts. *Sew. Ind. Wastes* **1953**, 802−839.
(28) Griffin, J. M.; West, J. L. Acute Toxicity of Ammonia-Base Neutral Sulfite Pulp Mill Waste Liquor to Rainbow Trout. *Bull. Environ. Contam. Toxicol.* **1976**, *15*, 608−612.
(29) Aquilina, G.; Bampidis, V.; Bastos, M. D. L.; Costa, L. G.; Flachowsky, G.; Gralak, M. A.; Hogstrand, C.; Leng, L.; Lopez-Puente, S.; Martelli, G. Scientific Opinion on the Safety and Efficacy of Lignosulphonate as a Feed Additive for All Animal Species. *EFSA J.* **2015**, *13*, 4160.
(30) Pharmacopeia, U. S. *Food Chemicals Codex*; 2008.
(31) Crestini, C.; Lange, H.; Sette, M.; Argyropoulos, D. S. On the Structure of Softwood Kraft Lignin. *Green Chem.* **2017**, *19*, 4104−4121.
(32) Sette, M.; Wechselberger, R.; Crestini, C. Elucidation of Lignin Structure by Quantitative 2D NMR. *Chem. − Eur. J.* **2011**, *17*, 9529−9535.
(33) Jeong, H.; Park, J.; Kim, S.; Lee, J.; Ahn, N. Compressive Viscoelastic Properties of Softwood Kraft Lignin-Based Flexible Polyurethane Foams. *Fibers Polym.* **2013**, *14*, 1301−1310.
(34) Li, J.; Henriksson, G.; Gellerstedt, G. Lignin Depolymerization/Repolymerization and Its Critical Role for Delignification of Aspen Wood by Steam Explosion. *Bioresour. Technol.* **2007**, *98*, 3061−3068.
(35) Duval, A.; Lawoko, M. A Review on Lignin-Based Polymeric, Micro-and Nano-Structured Materials. *React. Funct. Polym.* **2014**, *85*, 78−96.
(36) Guerra, A.; Gaspar, A. R.; Contreras, S.; Lucia, L. A.; Crestini, C.; Argyropoulos, D. S. On the Propensity of Lignin to Associate: A Size Exclusion Chromatography Study with Lignin Derivatives Isolated from Different Plant Species. *Phytochemistry* **2007**, *68*, 2570−2583.
(37) Lee, R. A.; Bédard, C.; Berberi, V.; Beauchet, R.; Lavoie, J.-M. UV−Vis as Quantification Tool for Solubilized Lignin Following a Single-Shot Steam Process. *Bioresour. Technol.* **2013**, *144*, 658−663.
(38) Bartzoka, E. D. *Ultrasound Assisted Development of Polyphenol Micro-Capsules for Controlled Active Delivery*. Thesis in Materials for Health, Environment and Energy, Università degli studi di Roma "Tor Vergata," 2017.
(39) Lucas, X.; Bauzá, A.; Frontera, A.; Quinonero, D. A Thorough Anion−π Interaction Study in Biomolecules: On the Importance of Cooperativity Effects. *Chem. Sci.* **2016**, *7*, 1038−1050.
(40) Hatefi, Y.; Hanstein, W. G. [77] Destabilization of Membranes with Chaotropic Ions. *Methods Enzymol.* **1974**, *31*, 770−790.
(41) Sharp, K. A.; Honig, B. Electrostatic Interactions in Macromolecules: Theory and Applications. *Annu. Rev. Biophys. Biophys. Chem.* **1990**, *19*, 301−332.
(42) McPhail, A. T.; Sim, G. A. Hydroxyl−Benzene Hydrogen Bonding: An X-Ray Study. *Chem. Commun. (London)* **1965**, 124−126.
(43) Lindberg, J. J.; Kuusela, T. A.; Levon, K. *Specialty Polymers from Lignin*; ACS Publications, 1989.
(44) Kunz, W.; Henle, J.; Ninham, B. W. 'Zur Lehre von Der Wirkung Der Salze'(about the Science of the Effect of Salts): Franz Hofmeister's Historical Papers. *Curr. Opin. Colloid Interface Sci.* **2004**, *9*, 19−37.
(45) Hyde, A. M.; Zultanski, S. L.; Waldman, J. H.; Zhong, Y.-L.; Shevlin, M.; Peng, F. General Principles and Strategies for Salting-Out Informed by the Hofmeister Series. *Org. Process Res. Dev.* **2017**, *21*, 1355−1370.
(46) Peruzzi, N.; Ninham, B. W.; Lo Nostro, P.; Baglioni, P. Hofmeister Phenomena in Nonaqueous Media: The Solubility of Electrolytes in Ethylene Carbonate. *J. Phys. Chem. B* **2012**, *116*, 14398−14405.
(47) Lo Nostro, P.; Ninham, B. W. Hofmeister Phenomena: An Update on Ion Specificity in Biology. *Chem. Rev.* **2012**, *112*, 2286−2322.
(48) Hatefi, Y.; Hanstein, W. G. Solubilization of Particulate Proteins and Nonelectrolytes by Chaotropic Agents. *Proc. Natl. Acad. Sci.* **1969**, *62*, 1129−1136.
(49) Hofmeister, F. Zur Lehre von Der Wirkung Der Salze. *Naunyn-Schmiedeberg's Arch. Pharmacol.* **1888**, *25*, 1−30.
(50) Collins, K. D. Charge Density-Dependent Strength of Hydration and Biological Structure. *Biophys. J.* **1997**, *72*, 65−76.
(51) Ninham, B. W.; Lo Nostro, P. *Molecular Forces and Self Assembly: In Colloid, Nano Sciences and Biology*; Cambridge University Press, 2010, DOI: 10.1017/CBO9780511811531.
(52) Moelbert, S.; Normand, B.; De Los Rios, P. Kosmotropes and Chaotropes: Modelling Preferential Exclusion, Binding and Aggregate Stability. *Biophys. Chem.* **2004**, *112*, 45−57.
(53) Zhang, Y.; Cremer, P. S. Interactions between Macromolecules and Ions: The Hofmeister Series. *Curr. Opin. Chem. Biol.* **2006**, *10*, 658−663.
(54) Rosen, M. J.; Kunjappu, J. T. *Surfactants and Interfacial Phenomena*; John Wiley & Sons, 2012, DOI: 10.1002/9781118228920.
(55) Rosen, M. J.; Kunjappu, J. T. Characteristic Features of Surfactants. *Surfactants Interfacial Phenom. Fourth Ed.* **2012**, *3*, 1−38.
(56) Bilanicová, D.; Salis, A.; Ninham, B. W.; Monduzzi, M. Specific Anion Effects on Enzymatic Activity in Nonaqueous Media. *J. Phys. Chem. B* **2008**, *112*, 12066−12072.
(57) Hallsworth, J. E.; Heim, S.; Timmis, K. N. Chaotropic Solutes Cause Water Stress in Pseudomonas Putida. *Environ. Microbiol.* **2003**, *5*, 1270−1280.

DOI: 10.1021/acsomega.8b03510
ACS Omega 2019, 4, 6979−6993

(58) McMaster, M. C. *HPLC: A Practical User's Guide*; John Wiley & Sons, 2007, DOI: 10.1002/0470079096.
(59) Ragnar, M.; Lindgren, C. T.; Nilvebrant, N.-O. PKa-Values of Guaiacyl and Syringyl Phenols Related to Lignin. *J. Wood Chem. Technol.* **2000**, *20*, 277−305.

DOI: 10.1021/acsomega.8b03510
ACS Omega 2019, 4, 6979−6993